RESIDUAL-GATED ATTENTION U-NET WITH CHANNEL RECALIBRATION FOR POLYP SEGMENTATION IN COLONOSCOPY IMAGES

William Tanuwijaya[1], Yohannes[2]
Faculty of Computer Science and Engineering, Universitas Multi Data Palembang
Jln. Rajawali No.14, 9 ilir, Kec. Ilir Timur 1, Palembang, Sumatera Selatan 30113
email williamtanuwijaya_2226250012@mhs.mdp.ac.id, yohannesmasterous@mdp.ac.id[2]

Abstract - This study proposed a modification to the Attention U-Net architecture by integrating a Residual-Gated mechanism and Squeeze-and-Excitation (SE) Block based channel recalibration within the Attention Gate to enchance feature selectivity in polyp segmentation. This integration reinforces both spatial and channel attention, enabling the model to better highlight polyp regions while suppressing irrelevant background features. Experiments were conducted on three colonoscopy datasets CVC-ClinicDB, CVC-ColonDB, and CVC-300 using IoU and DSC metrics. Compared to the Attention U-Net baseline, the proposed model achieves noticeable improvements, with performance gains of mIoU 00043 and mDSC 0.0094 on CVC-ClinicDB, mIoU 0.0012 on CVC-ColonDB, and a larger margin of mIoU 0.0224 and mDSC 0.0127 on CVC-300. The best results were obtained on CVC-ClinicDB (mIoU 0.8889, mDSC 0.9412). Although the absolute scores on CVC-ClinicDB and CVC-ColonDB are lower than those reported in several recent studies, these datasets contain higher variability in polyp size, boundary ambiguity, and illumination, contributing to more challenging segmentation conditions. Visual evaluation further shows smoother and more coherent boundaries, especially on small or low contras polyps. Overall, the integration of the Residual-Gated mechanism and SE Block within the Attention Gate effectively improves model accuracy and generalization, particulary in challenging scenarios.

Keywords – Attention U-Net; Channel Recalibration; Colorectal Polyp Segmentation; Residual-Gated Mechanism; Squeeze-and-Excitation Block.

I. INTRODUCTION

Colorectal cancer is a serious cancer of the digestive system characterized by the growth of malignant cells in the colon. This condition generally begins with the formation of polyps or benign tumors, which may gradually develop into cancer over time [1], [2]. Reports from the International Agency for Research on Cancer (IARC) indicate that colorectal cancer ranks second as the leading cause of cancer-related deaths worldwide, with more than 900,000 fatalities each year [3]. Therefore, early detection of polyps through colonoscopy remains crucial to prevent progression toward colorectal cancer [4]. However, automatic polyp detection and segmentation remain challenging due to variations in polyp shapes, sizes, and colors, non-uniform illumination, the presence of specular highlights, and blurred boundaries that appear in colonoscopy images [5], [6]. In clinical settings, small or low-contrast polyps may even be missed during screening procedures [7]. With the rapid advancement of artificial intelligence, deep learning based methods have become widely used to improve segmentation performance in colonoscopy images [8]. Among these, the Attention U-Net architecture introduces an attention gate (AG) mechanism that filters irrelevant background features while preserving salient structures [9]. This model is evaluated in this study using three colonoscopy datasets CVC-300 [10], CVC-ColonDB [11], and CVC-ClinicDB [12] with IoU and DSC as evaluation metrics [13], [14].

Attention U-Net has been shown to outperform the standard U-Net in medical image segmentation, including pancreas, spleen, and kidney segmentation tasks, with improvements of 2-3% in DSC across organs [9]. Meanwhile, the Squeeze-and-Excitation (SE) Block [15] enhances channel-wise feature representation by modeling inter-channel dependencies through squeeze-and-excitation

operations. The Attention Gate (AG) itself serves to suppress irrelevant responses and focus on spatially important regions [9]. Residual connections, introduced in ResNet [16], provide stable gradient flow and enable deeper architectures by learning residual mappings instead of direct transformations [17]. Several studies have attempted to improve polyp segmentation by modifying the U-Net backbone. Research by [18] reported DSC 0.799 on CVC-ClinicDB, while [19] achieved DSC 0.7217 on Kvasir-SEG. Research by [20] integrated SE Blocks into the encoder and decoder to strengthen channel recalibration, and [21] introduced residual blocks to preserve structural information and stabilize the gradient flow. Although these approaches demonstrate improvements, they primarily insert SE and Residual modules in encoder-decoder pathways, not inside the attention mechanism itself.

II. STUDY SIGNIFICANCE

This study uses CVC-ClinicDB (612 images), CVC-ColonDB (380 images), and CVC-300 (60 images) datasets. The datasets can be seen in Figure 1.

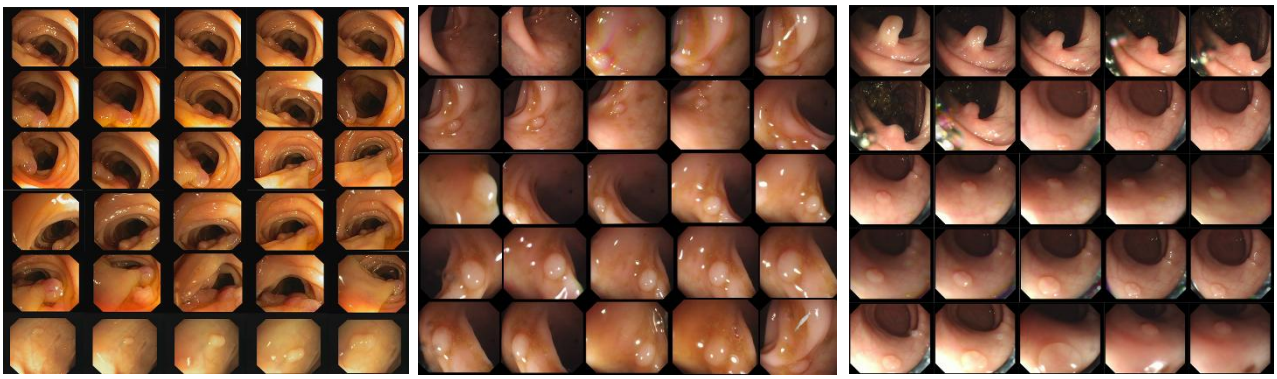

(a) **(b)** **(c)**

Figure 1. Research Datasets: **(a)**. CVC-ClinicDB **(b)**. CVC-ColonDB **(c)**. CVC-300.

In this study, model development began with dataset preparation involving three publicly available colonoscopy dataset CVC-ClinicDB, CVC-ColonDB, and CVC-300. Following the preprocessing protocol in [11], all images were resized to 352 × 352 pixels [22], and data augmentation included horizontal and vertical flipping, random rotations between -10° and 10°, and random scaling ±10%. This augmentation strategy was intentionally selected to simulate variations in polyp orientation, size, and illumination while avoiding excessive distortion that could harm boundary preservation.

The model training process used a learning rate [23] of 1×10^{-4}, the AdamW optimizer [4], a batch size of 16, and 100 training epochs [11]. This configuration was applied not only to maintain consistency with previous studies but also because preliminary observations showed that higher learning rates caused unstable attention responses, whereas lower learning rates slowed convergence. A batch size of 16 provided stable gradients without over-smoothing, and 100 epochs were sufficient for the model to reach convergence [24]. The model used in this study is Attention U-Net, which was developed to improve the ability to segment polyp areas. In addition, the dataset was divided into 80% training data, 10% validation data, and 10% test data to ensure balanced learning and reliable performance monitoring [25].

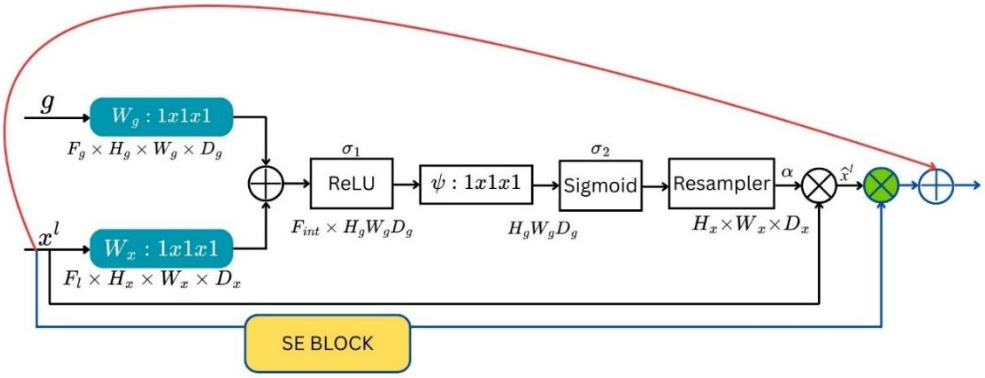

Figure 2. Architecture Residual-Gated and SE Block in Attention Gate

Specifically in Figure 2, the Attention Gate mechanism is implemented by integrating both the SE Block and a Residual Connection directly within the gating pipeline. The process begins by projecting the gating signal g and the skip-connection feature x^l through separate 1 × 1 convolutions to match their channel dimensions, producing tensors of identical shape. These projected features are then fused through element-wise addition and passed through a ReLU activation to generate the intermediate representation F_{int}. The attention coefficients are computed by applying a 1 × 1 convolution ψ followed by a Sigmoid activation, yielding the spatial attention map α. Because the spatial resolution of g and x^l may differ, the attention map is resampled using bilinear interpolation to align it with the skip feature. After spatial gating, the SE Block performs channel recalibration by applying global average pooling followed by two fully connected layers and a Sigmoid function, producing channel weights that modulate the gated feature map. Finally, the recalibrated attention output is multiplied element-wise [26] with x^l and merged with g through a residual connection to stabilize training and preserve fine structural details. The resulting feature map is then forwarded to the next decoder stage, as illustrated in Figure 3.

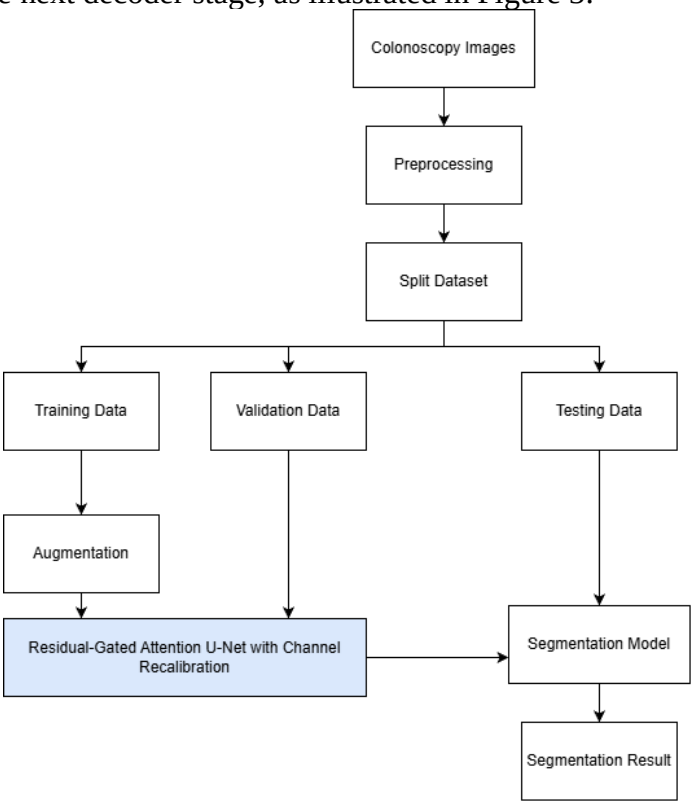

Figure 3. Model design scheme

Metrics used are IoU and DSC. IoU is an evaluation metric used assess degree of agreement between prediction results (A) and the ground truth (B), particularly in object detection and image

segmentation tasks [5]. The IoU value ranges from [0, 1], where a value close to 1 indicates a high level of agreement between prediction and ground truth, while a value close to 0 indicates a low level of agreement [27]. Mathematically, IoU is formulated in Equation (1).

$$IoU = \frac{A \cap B}{A \cup B} = \frac{TP}{TP + FP + FN} \tag{1}$$

DSC in an evalution metric used to assess segmentation performance in medical images. This metric measures degree of similarity or overlap between predicted segmentation result (A) and the ground truth (B) [28]. The DSC value ranges from [0, 1], where a value of 1 indicates perfect agreement between predicted results and ground truth, while a value of 0 indicates no overlap at all [27]. Mathematically, DSC if formulated in Equation (2).

$$DSC = \frac{2 \times |A \cap B|}{|A| + |B|} = \frac{2 \times TP}{2 \times TP + FP + FN} \tag{2}$$

III. RESULT AND DISCUSSION

This study consists of four testing scenarios: U-Net [29], Attention U-Net [9], Residual-Gated Attention U-Net, and the proposed Residual-Gated Attention U-Net with Channel Recalibration.

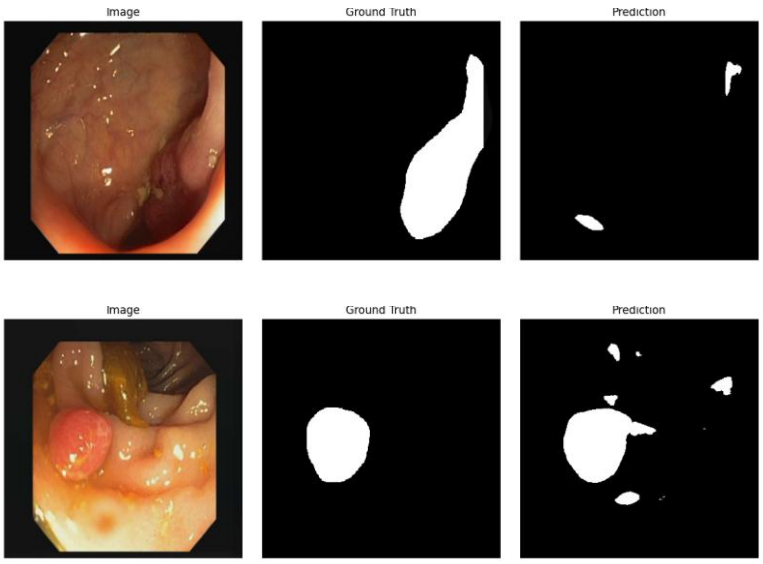

Figure 4. Result CVC-ClinicDB

Figure 4 shows the segmentation results on the CVC-ClinicDB dataset. Visually, the proposed model produces smoother and more stable boundaries, even on low-contrast or blurred polyps, indicating that the integration of residual gating and SE-based channel recalibration strengthens feature selectivity. These observations are consistent with the quantitative improvements in Table 1 and Table 2.

Table 1. Result Train CVC-ClinicDB

No.	Methods	mIoU	mDSC
1.	U-Net	0.82011	0.900765
2.	Attention U-Net	0.81855	0.899089
3.	Residual-Gated Attention U-Net	0.811113	0.895247
4.	Residual-Gated Attention U-Net with Channel Recalibration **(Ours)**	0.842263	0.914197

Table 1 presents the training results on the CVC-ClinicDB dataset. The proposed model achieves an mIoU of 0.842263 and an mDSC of 0.914197, the highest among all baselines. U-Net and Attention U-Net show relatively similar performance, while the Residual-Gated Attention U-Net without SE Block experiences a decline due to unstable gating sensitivity. The improvement obtained by the proposed model indicates that channel recalibration inside the Attention Gate effectively strengthens feature selectivity during training. However, this strong training performance also contrasts sharply with the lower test results shown in Table 2, suggesting the presence of a train–test distribution gap. Factors such as high variation in polyp texture, illumination differences, and limited augmentation diversity likely contribute to reduced generalization when the model is evaluated on unseen images.

Table 2. Result Test CVC-ClinicDB

No.	Methods	mIoU	mDSC
1.	U-Net	0.1713	0.2719
2.	Attention U-Net	0.2340	0.3721
3.	Residual-Gated Attention U-Net	0.1343	0.2358
4.	Residual-Gated Attention U-Net with Channel Recalibration **(Ours)**	0.2383	0.3815

Table 2 shows the test results on the CVC-ClinicDB dataset. The proposed model again achieves the best performance with an mIoU of 0.2383 and an mDSC of 0.3815. Although all models experience a substantial decrease in accuracy compared to their training scores, this decline is expected due to the high variability in polyp appearance across the dataset, including differences in texture, illumination, and boundary clarity. These factors create a distribution shift between training and test samples, resulting in reduced generalization. Even under these conditions, the proposed model remains the most robust, with Attention U-Net ranking second, indicating that the attention mechanism still provides meaningful benefits. Meanwhile, the weaker performance of the Residual-Gated Attention U-Net without SE Block highlights the importance of channel recalibration in stabilizing the attention response on unseen data.

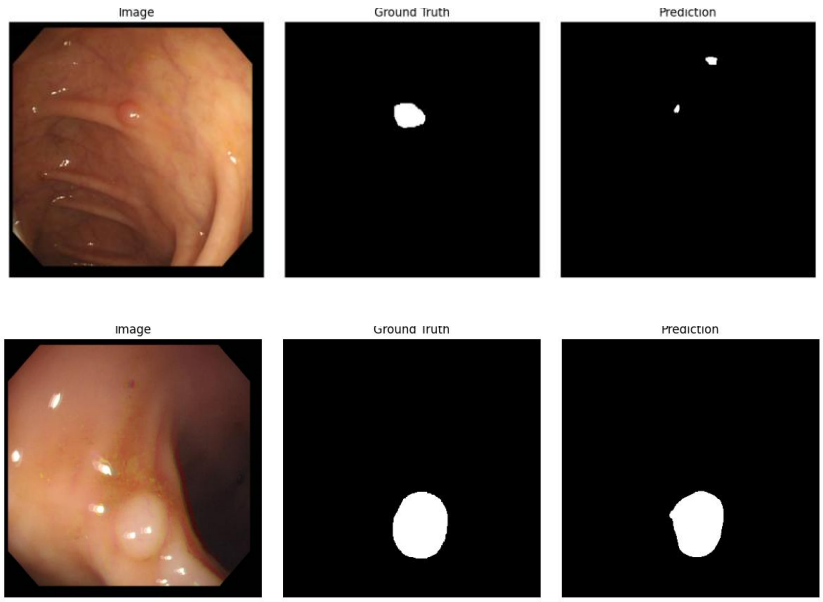

Figure 5. Result CVC-ColonDB

Figure 5 shows the segmentation results on the CVC-ColonDB dataset using the proposed model. Although this dataset exhibits substantial variation in mucosal texture, illumination, and global appearance, the model is still able to identify polyp regions consistently. In several examples, small polyps with low contrast or unclear boundaries can still be segmented without excessive region expansion, demonstrating that the combination of the residual connection and SE Block inside the

Attention Gate helps strengthen spatial feature discrimination and reduce irrelevant background activation. These visual results correspond with the improvements reported in Table 3 and Table 4. However, some challenging cases also reveal the model's limitations, such as missed detection of very small polyps or false positives on mucosal folds, indicating that the high variability in this dataset continues to affect generalization despite the enhanced gating mechanism.

Table 3. Result Train CVC-ColonDB

No.	Methods	mIoU	mDSC
1.	U-Net	0.679258	0.802372
2.	Attention U-Net	0.704844	0.816174
3.	Residual-Gated Attention U-Net	0.630776	0.763352
4.	Residual-Gated Attention U-Net with Channel Recalibration **(Ours)**	0.612025	0.75585

Table 3 shows that for the training data, Attention U-Net achieves the highest performance with an mIoU of 0.704844 and an mDSC of 0.816174. Interestingly, the proposed model records lower training values, with an mIoU of 0.612025 and an mDSC of 0.75585. This behavior is consistent with the effect of the SE Block, which enforces stronger channel selectivity and prevents the model from memorizing redundant or noisy features. As a result, the proposed architecture becomes less prone to overfitting on the highly variable textures and illumination patterns present in CVC-ColonDB. The slightly lower training scores therefore indicate a more controlled fitting process, which aligns with the improved test performance shown in Table 4.

Table 4. Result Test CVC-ColonDB

No.	Methods	mIoU	mDSC
1.	U-Net	0.1847	0.2984
2.	Attention U-Net	0.2442	0.3810
3.	Residual-Gated Attention U-Net	0.1721	0.2867
4.	Residual-Gated Attention U-Net with Channel Recalibration **(Ours)**	0.2454	0.3803

Table 4 shows that the proposed model achieves an mIoU of 0.2454 and an mDSC of 0.3803, making it the best-performing method on the CVC-ColonDB test set. These results support the earlier interpretation that channel recalibration helps the model generalize better to previously unseen images. Attention U-Net ranks second with performance close to that of the proposed model, indicating that spatial attention alone already provides a meaningful advantage. The lower performance of the Residual-Gated Attention U-Net without channel recalibration suggests that the residual-gated mechanism, when used alone, is not stable enough to handle the substantial texture and illumination variations in this dataset. Overall, the relatively modest test scores across all models also reflect the high complexity and distribution variability of CVC-ColonDB, which pose challenges for generalization despite strong training results.

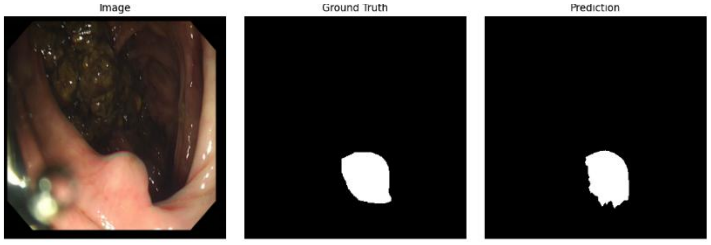

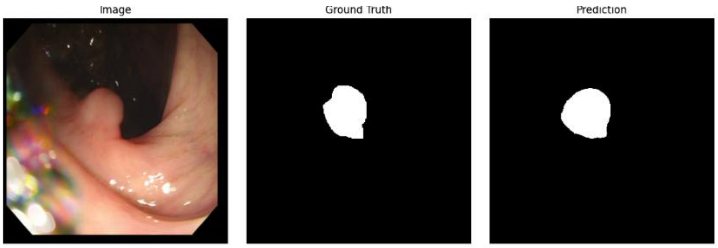

Figure 6. Result CVC-300

Figure 6 shows the segmentation results on the CVC-300 dataset, which contains a relatively small number of images. Despite the limited dataset size, the proposed model produces accurate segmentation with clear polyp boundaries and minimal region overestimation. This suggests that the channel recalibration mechanism helps regulate feature sensitivity, allowing the model to avoid overfitting and maintain stable predictions. The consistency between the training and testing visual results aligns with the high mIoU and mDSC values reported in Table 5 and Table 6. Nevertheless, a few cases with extremely low-contrast polyps still pose challenges, indicating that even on smaller datasets, boundary ambiguity remains a potential source of error.

Table 5. Result Train CVC-300

No.	Methods	mIoU	mDSC
1.	U-Net	0.794467	0.885463
2.	Attention U-Net	0.866503	0.928478
3.	Residual-Gated Attention U-Net	0.706398	0.82794
4.	Residual-Gated Attention U-Net with Channel Recalibration **(Ours)**	0.888889	0.941176

Table 5 shows that on the training data, the proposed model achieves an mIoU of 0.888889 and an mDSC of 0.941176, outperforming all comparison models. Attention U-Net ranks second with slightly lower accuracy. These results confirm that on small datasets such as CVC-300, the integration of residual gating and channel recalibration provides stronger fitting capability while still maintaining stable optimization.

Table 6. Result Test CVC-300

No.	Methods	mIoU	mDSC
1.	U-Net	0.7937	0.8850
2.	Attention U-Net	0.8665	0.9285
3.	Residual-Gated Attention U-Net	0.7064	0.8279
4.	Residual-Gated Attention U-Net with Channel Recalibration **(Ours)**	0.8889	0.9412

Table 6 shows that the proposed model is again the best-performing method, with an mIoU of 0.8889 and an mDSC of 0.9412, identical to the training results. The stability between the train and test values indicates that the proposed model generalizes well on small datasets, where the distribution gap between training and testing samples is relatively limited. In contrast, all other baselines show lower performance and a noticeable imbalance between their train and test scores, particularly the Residual-Gated Attention U-Net without channel recalibration, which appears to underfit. These results suggest that the integration of residual gating and SE-based channel recalibration is especially effective in maintaining consistent performance on compact datasets, although broader validation on more diverse data remains necessary for stronger generalization claims. Despite the improvements observed across individual experiments, a clear performance gap is visible between the training and testing results in both CVC-ClinicDB and CVC-ColonDB. The substantial drop in mIoU and mDSC during testing is mainly caused by the high variability in polyp size, illumination, mucosal texture, and boundary clarity, which create a distribution shift relative to the training samples. Although the augmentation strategy introduces basic geometric variations, it may not sufficiently capture the full complexity of these datasets, resulting in reduced generalization capability. These observations

indicate that while the proposed residual-gated and channel-recalibrated Attention Gate provides measurable improvements, further architectural refinements, richer augmentation strategies, and multi-run evaluations are needed to achieve more stable and clinically reliable performance.

IV. CONCLUSIONS

This study proposes a Residual-Gated Attention U-Net with Channel Recalibration by integrating a residual connection mechanism [16] and an SE Block [15] directly into the Attention Gate. This design enhances both spatial and channel selectivity, enabling the model to better highlight polyp regions and suppress irrelevant background features. Experiments conducted on three colonoscopy datasets CVC-ClinicDB, CVC-ColonDB, and CVC-300 demonstrate consistent performance improvements over the baseline Attention U-Net in terms of mIoU, mDSC, and visual boundary quality, particularly for small, low-contrast, or blurred polyps. These findings indicate that combining residual gating with channel recalibration effectively strengthens the attention mechanism and enhances generalization on both complex and limited-data scenarios. Despite these improvements, several limitations remain. The overall performance is still lower than that of recent transformer-based state-of-the-art (SOTA) models, indicating room for further architectural enhancement. The evaluation is restricted to three 2D still-image datasets and does not include video-based or real-time settings, which are crucial for clinical deployment. Moreover, the model has not been validated in actual clinical environments, and therefore its reliability for use as a Computer-Aided Diagnosis (CAD) tool cannot yet be established. These constraints highlight the need for broader dataset diversity, more comprehensive testing scenarios, and stronger experimental validation. Future research should explore larger and more heterogeneous datasets, extend evaluation to real-time colonoscopy videos, and include clinical testing to assess practical utility. Investigating loss functions tailored for small polyp detection and optimizing computational efficiency to support real-time inference also represent important directions for further development.

REFERENCES

[1] F. Du, Z. Wang, J. C. M. Than, H. N. Afrouzi, and N. Qian, "DoubleAANet: Auxiliary attention and area adaptive loss for robust polyp segmentation," *J. Comput. Des. Eng.*, vol. 12, no. 8, pp. 1–13, 2025, doi: 10.1093/jcde/qwaf061.

[2] P. Li, J. Ding, and C. S. Lim, "VMDU-net: a dual encoder multi-scale fusion network for polyp segmentation with Vision Mamba and Cross-Shape Transformer integration," *Front. Artif. Intell.*, vol. 8, no. June, pp. 1–18, Jun. 2025, doi: 10.3389/frai.2025.1557508.

[3] IARC, "Colorectal Cancer," *International Agency for Research on Cancer*, 2022. https://www.iarc.who.int/cancer-type/colorectal-cancer/ (accessed Sep. 02, 2025).

[4] L. Jiang, Y. Hui, Y. Fei, Y. Ji, and T. Zeng, "Improving Polyp Segmentation with Boundary-Assisted Guidance and Cross-Scale Interaction Fusion Transformer Network," *Processes*, vol. 12, no. 5, p. 1030, May 2024, doi: 10.3390/pr12051030.

[5] X. Liu, N. A. M. Isa, C. Chen, and F. Lv, "Colorectal Polyp Segmentation Based on Deep Learning Methods: A Systematic Review," *J. Imaging*, vol. 11, no. 9, p. 293, Aug. 2025, doi: 10.3390/jimaging11090293.

[6] K. ELKarazle, V. Raman, C. Chua, and P. Then, "RetSeg: Retention-based Colorectal Polyps Segmentation Network," Mar. 2024, [Online]. Available: http://arxiv.org/abs/2310.05446.

[7] X. Cao, K. Fan, C. Xu, H. Ma, and K. Jiao, "CMNet: deep learning model for colon polyp segmentation based on dual-branch structure," *J. Med. Imaging*, vol. 11, no. 02, pp. 1–14, 2024, doi: 10.1117/1.jmi.11.2.024004.

[8] I. Malli, I. A. Vezakis, I. Kakkos, T. Kalamatianos, and G. K. Matsopoulos, "Unsupervised Domain Adaptation for Automatic Polyp Segmentation Using Synthetic Data," *Appl. Sci.*, vol. 15, no. 17, p. 9829, Sep. 2025, doi: 10.3390/app15179829.

[9] O. Oktay *et al.*, "Attention U-Net: Learning Where to Look for the Pancreas," in *1st Conference on Medical Imaging with Deep Learning (MIDL 2018), Amsterdam, The Netherlands*, May 2018, no. Midl, doi: https://doi.org/10.48550/arXiv.1804.03999.

[10] M. Mansoori, S. Shahabodini, J. Abouei, K. N. Plataniotis, and A. Mohammadi, "Polyp SAM 2: Advancing Zero shot Polyp Segmentation in Colorectal Cancer Detection," *arXiv*, pp. 0–6, 2024, [Online]. Available: http://arxiv.org/abs/2408.05892.
[11] X. Xie and X. Shen, "Polyp Segmentation Algorithm Based on the Dual Attention and Fusion Mechanism," *Electronics*, vol. 14, no. 12, p. 2316, Jun. 2025, doi: 10.3390/electronics14122316.
[12] J. Bernal, F. J. Sánchez, G. Fernández-Esparrach, D. Gil, C. Rodríguez, and F. Vilariño, "WM-DOVA maps for accurate polyp highlighting in colonoscopy: Validation vs. saliency maps from physicians," *Comput. Med. Imaging Graph.*, vol. 43, pp. 99–111, Jul. 2015, doi: 10.1016/j.compmedimag.2015.02.007.
[13] Y. Tong, Z. Chen, Z. Zhou, Y. Hu, X. Li, and X. Qiao, "An Edge-Enhanced Network for Polyp Segmentation," *Bioengineering*, vol. 11, no. 10, pp. 1–19, 2024, doi: 10.3390/bioengineering11100959.
[14] M. F. Ahamed *et al.*, "IRv2-Net: A Deep Learning Framework for Enhanced Polyp Segmentation Performance Integrating InceptionResNetV2 and UNet Architecture with Test Time Augmentation Techniques," *Sensors*, vol. 23, no. 18, 2023, doi: 10.3390/s23187724.
[15] J. Hu, L. Shen, and G. Sun, "Squeeze-and-Excitation Networks," in *2018 IEEE/CVF Conference on Computer Vision and Pattern Recognition*, Jun. 2018, pp. 7132–7141, doi: 10.1109/CVPR.2018.00745.
[16] K. He, X. Zhang, S. Ren, and J. Sun, "Deep Residual Learning for Image Recognition," in *2016 IEEE Conference on Computer Vision and Pattern Recognition (CVPR)*, Jun. 2016, vol. 2016-Decem, pp. 770–778, doi: 10.1109/CVPR.2016.90.
[17] J. Raymann and R. Rajalakshmi, "GAR-Net: Guided Attention Residual Network for Polyp Segmentation from Colonoscopy Video Frames," *Diagnostics*, vol. 13, no. 1, p. 123, Dec. 2022, doi: 10.3390/diagnostics13010123.
[18] A. Santone, M. Cesarelli, and F. Mercaldo, "A Method for Polyp Segmentation Through U-Net Network," *Bioengineering*, vol. 12, no. 3, p. 236, Feb. 2025, doi: 10.3390/bioengineering12030236.
[19] W. H. Rafi, M. D. Sulistiyo, S. Hadiyoso, and U. N. Wisesty, "Polyp Identification from a Colonoscopy Image Using Semantic Segmentation Approach," *Build. Informatics, Technol. Sci.*, vol. 5, no. 2, pp. 423–431, 2023, doi: 10.47065/bits.v5i2.4083.
[20] L. Rundo *et al.*, "USE-Net: Incorporating Squeeze-and-Excitation blocks into U-Net for prostate zonal segmentation of multi-institutional MRI datasets," *Neurocomputing*, vol. 365, pp. 31–43, Nov. 2019, doi: 10.1016/j.neucom.2019.07.006.
[21] L. Xiang, Y. Li, W. Lin, Q. Wang, and D. Shen, "Unpaired Deep Cross-Modality Synthesis with Fast Training," in *Springer*, vol. 11045, D. Stoyanov, Z. Taylor, G. Carneiro, T. Syeda-Mahmood, A. Martel, L. Maier-Hein, J. M. R. S. Tavares, A. Bradley, J. P. Papa, V. Belagiannis, J. C. Nascimento, Z. Lu, S. Conjeti, M. Moradi, H. Greenspan, and A. Madabhushi, Eds. Cham: Springer International Publishing, 2018, pp. 155–164.
[22] R. Ghimire and S. W. Lee, "MMNet: A Mixing Module Network for Polyp Segmentation," *Sensors*, vol. 23, no. 16, pp. 1–16, 2023, doi: 10.3390/s23167258.
[23] P. Desiana, W. Ayu, and G. A. Pradipta, "Analisis Performansi Parameter pada Arsitektur U-Net untuk Segmentasi Nukleus pada Citra Kanker Serviks," pp. 131–138, 2024, doi: https://doi.org/10.30864/jsi.v18i2.607.
[24] H. Li, D. Zhang, J. Yao, L. Han, Z. Li, and J. Han, "ASPS: Augmented Segment Anything Model for Polyp Segmentation," *Lect. Notes Comput. Sci. (including Subser. Lect. Notes Artif. Intell. Lect. Notes Bioinformatics)* , vol. 15009 LNCS, pp. 118–128, 2024, doi: 10.1007/978-3-031-72114-4_12.
[25] Z. Ji *et al.*, "LightCF-Net: A Lightweight Long-Range Context Fusion Network for Real-Time Polyp Segmentation," *Bioengineering*, vol. 11, no. 6, 2024, doi: 10.3390/bioengineering11060545.
[26] G. Feng, "Element-wise Attention Is All You Need," *arXiv*, 2025, doi: https://doi.org/10.48550/arXiv.2501.05730.
[27] Sonia and Yohannes, "Penerapan Model U-Net untuk Segmentasi Gigi pada Citra Radiografi Panoramik Orang Dewasa," vol. 5, no. 2, pp. 188–198, 2025, doi: https://doi.org/10.35957/algoritme.v5i2.10965.
[28] X. Zheng, W. Gong, R. Yang, and G. Zuo, "Image Segmentation of Intestinal Polyps using Attention Mechanism based on Convolutional Neural Network," *Int. J. Adv. Comput. Sci. Appl.*, vol. 14, no. 1, pp. 586–593, 2023, doi: 10.14569/IJACSA.2023.0140164.
[29] O. Ronneberger, P. Fischer, and T. Brox, "U-Net: Convolutional Networks for Biomedical Image Segmentation BT - Medical Image Computing and Computer-Assisted Intervention – MICCAI 2015," 2015, pp. 234–241.